A Hybrid Model of PSO Algorithm and Artificial Neural Network for Automatic Follicle Classification

O. R. Isah[1,*], A. D. Usman[2], A. M. S. Tekanyi[3]

[1]*Department of Computer Engineering*
Federal University of Technology
Minna, Niger State, P.M.B. 65, Nigeria
E-mail: Isah.rabiu@futminna.edu.ng

[2]*Department of Electrical/Electronic Engineering*
Kaduna Polytechnic, Kaduna, Kaduna State, Nigeria
E-mail: aliyu_d_usman@yahoo.com

[3]*Department of Electrical/Computer Engineering*
Ahmadu Bello University, Zaria, Nigeria
E-mail: amtekanyi@abu.edu.ng

[*]*Corresponding author*

Received: July 21, 2016 **Accepted: February 16, 2017**

Published: March 31, 2017

Abstract: *Polycystic Ovarian Syndrome (PCOS) is one of the leading causes of infertility in the world, but is a preventable disease when detected early. Detection of follicles in ultrasound images of the ovary is required for the diagnosis of PCOS. The manual method of detecting follicles is time consuming, laborious, error-prone and inconvenient for patients. However, methods used by the existing automated systems often lead to a reduction in accuracy, sensitivity and specificity due to the irregular and jagged edges of the follicles. This research work aims at achieving an improved specificity, sensitivity and accuracy of the system. In this report, a new technique for the automatic detection of follicles is implemented. Lee filter was used to despeckle the ultrasound images. Multiple features were then extracted from the images. Further, twelve of these features were selected as optimal values by the Particle Swarm Optimization algorithm. Then, these features were fed as input to the Multilayer Perceptron Artificial Neural Network. Upon training and testing the network, 98.3% accuracy, 100% sensitivity and 96.8% specificity were achieved.*

Keywords: *Polycystic ovarian syndrome, Particle swarm optimization, False acceptance rate, False rejection rate, Follicle detection rate, Multi-layer perceptron artificial neural network.*

Introduction

Ultrasound imaging is the popular modality widely used for the visualization of women ovary with the aim of revealing various stages of follicular development for fertility treatment, early detection of Polycystic Ovarian Syndrome (PCOS) and ovarian cancer [28]. The widely usage of ultrasound machine is due to its non-invasive nature; moreover, it is easy to use, less expensive as well as painless and causing less discomfort compared to other imaging modalities [16]. However, accurate interpretations of these images by medical experts are always difficult due to the presence of image artefacts and speckle noise [16]. This is because the ovary contains tissues, blood vessels, and endometrium, which are all captured in the process of ultrasound scanning [26].

Polycystic Ovarian Syndrome (PCOS) is an abdominal disorder that causes diseases such as type 2 diabetes, ovarian cancer, hypertension and infertility among women of reproductive age [2]. Five (5%) to ten percent (10%) of these women are affected by PCOS worldwide [4]. Early diagnosis of PCOS is necessary to avert the future consequences it poses to women [15].

The manual method of classifying and diagnosing PCOS is labour-intensive, prone to error, time-consuming and inconvenient for both the patients and the physicians [25]. The automated techniques reduce the time for diagnosing and are less labour-intensive and more convenient, but the follicle detection rate needs to be improved for these techniques to work well with automated systems [25].

Image feature extraction is the process of extracting distinct features of the image that are relevant to the classification task [23]. Feature extraction technique transforms the input image into salient features called a feature vector by reducing image dimensionality [11]. This research adopted multiple features including geometric, first order texture and Gray Level Co-occurrence Matrix (GLCM) based features. The reason is to determine the optimal features that will give a high classification accuracy, using the Particle Swarm Optimization (PSO) algorithm.

PSO is a type of meta-heuristic algorithm based on a randomly selected population called particles [12]. The particles, associated with their velocities, move collectively in a search space in search of optimal solution [21]. The objective function to be optimized is used to evaluate the fitness values of the particles in PSO [21].

Artificial Neural Network (ANN) is a network of connecting neurons that mimic the functionality of the human brain [13]. It has the ability to solve non-linear and complex problems. Its wide usage in image processing is due to its abilities to learn complex and non-linear input-output functions, to process parallel information and to adapt to the varying environment data [13].

The aim of this research is to automate the classification of follicles through hybridized PSO algorithm and ANN. The objective is the quantification of multiple features, including geometric, first order texture and GLCM-based features, optimal features' selection using PSO and ANN classification based on the selected optimal features.

Materials and methods

In this section, the detailed procedures for the successful completion of this research are discussed.

Image feature extraction

Image feature extraction is the process of extracting distinct features of the image that are relevant to the classification task [3]. The feature extraction technique transforms the input image into salient features called a feature vector by reducing the image dimensionality [3].

Natural images consist of textured (coarseness, contrast, entropy, homogeneity) and un-textured (Area, perimeter, Euler number, bounding box, etc.) features [3] that provide geometric and structural information about an image [27]. This research adopts multiple features including geometric, first order texture and GLCM based features. The reason is to determine the optimal features that will give a high classification accuracy. The features are explained in the following subsections:

First order features

A histogram of gray-levels can give concise statistical first order information about an image [17]. This is because gray-level histograms are calculated using a single pixel [17]. The shape of the histogram portrays the characteristics of the image so that a narrowly-distributed shape of a histogram represents a low-contrast image. Parameters such as mean, variance, skewness, kurtosis, standard deviation, energy and entropy are derived from the histogram of the image [17].

Mean: The mean intensity value indicates the average intensity value of all the pixels that belong to the same region. The mean can be expressed mathematically as [17]:

$$\text{Mean} = \frac{1}{N}\sum_{k=1}^{N} Intensity(k), \tag{1}$$

where N is the total number of samples.

Standard Deviation (SD): SD is a measure of how much the gray-levels differ from the mean, defined by the [17]:

$$\text{SD} = \frac{1}{N}\sum_{k=1}^{N}\left(Mean(k) - Intensity(k)\right)^2. \tag{2}$$

Variance: The variance is the square of the standard deviation (SD) [8].

Skewness: Skewness is a measure of the asymmetry of the data around the sample mean. If the skewness is negative, the data are spread out more to the left of the mean than to the right. If the skewness is positive, the data are spread out more to the right [8]. The skewness of the normal distribution (or any perfectly symmetric distribution) is zero. The skewness of a distribution is defined as [8]:

$$s = \frac{E\left(x-\mu\right)^3}{\sigma^3}, \tag{3}$$

where E represents the expected value of the distribution; μ is the mean of x; σ is the standard deviation of x.

Kurtosis: Kurtosis is a measure of how outlier-prone a distribution is. The kurtosis of the normal distribution is three. Distributions that are more outlier-prone than the normal distribution have kurtosis greater than three; distributions that are less outlier-prone have kurtosis less than three [8]. The kurtosis of a distribution is defined as [8]:

$$k = \frac{E\left(x-\mu\right)^4}{\sigma^4}. \tag{4}$$

Energy: This feature measures the consistency of the intensity distribution level. The high value of the energy feature indicates that the distribution is to a small number of intensity levels [18]. The mathematical representation of this feature is given as [18]:

$$\text{Energy} = \frac{1}{MN}\sum_{x=1}^{M}\sum_{y=1}^{N} I^2(x,y). \quad (5)$$

The main strength of this approach is its simplicity and ease of implementation through the use of standard descriptors such as mean and variance.

Gray level co-occurrence matrix

The GLCM method, otherwise known as Gray-Tone Spatial Dependence Matrices (GTSDM), is used to extract second order textural features of an image [20]. The first framework for calculating GLCM was first developed by Nithya and Santhi [18]. It was assumed that textural information is sufficiently represented by GLCM of two adjacent pixels, *i* and *j*, the distance *d* between the pixels and the angular relationship θ between them given in a mathematical expression as [14]:

$$P(i, j : d, \theta). \quad (6)$$

GLCM describes the texture content of an image in the horizontal (0°), vertical (90°), right-diagonal (45°), and left-diagonal (135°) directions [14]. Haralick *et al.* [9], defines fourteen measures of textural features which are based on four fundamental textural features: Angular Second Moment (ASM) or Energy, Inverse Difference Moment (IDM) or Homogeneity, Contrast and Correlation. The definitions of these features are given as:

ASM: The ASM is also referred to as energy. It returns the sum of the squared element in GLCM. The value ranges from 0 to 1. It is given as [9]:

$$\text{ASM} = \sum_{i,j} p(i,j)^2, \quad (7)$$

where i and j are pixels' intensity values.

IDM or Homogeneity: The IDM measures how close to each other are the distribution elements in the GLCM. The mathematical expression is given as [9]:

$$\text{IDM} = \sum_{i,j} \frac{p(i,j)}{1+|i-j|}, \quad (8)$$

where i and j represent intensity values of adjacent pixels.

Contrast: It measures contrast intensity of adjacent pixels over the whole image. It is given as [9]:

$$\text{Contrast} = \sum_{i,j} |i-j|^2 p(i,j), \quad (9)$$

where i and j are gray intensity values of adjacent pixels.

Correlation: It measures the correlation of pixels over the whole image. Its value ranges from 1 to −1. It is given as [9]:

$$\text{Correlation} = \sum_{i,j} \frac{(i-\mu i)(j-\mu j)\,p(i,j)}{\sigma_i \sigma_j}, \quad (10)$$

where i and j represent gray-level values of adjacent pixels; μ is the mean; σ is the standard deviation of the image.

Geometric features

Geometric features are the shape characteristics of a given image that could be used in image processing for a classification task [6]. These features include Area, Eccentricity, Diameter, Major Axis Length, and Minor Axis Length. These features are defined as follows [6]:

Area: The actual number of pixels in the region.

Eccentricity: The eccentricity is the ratio of the distance between the foci of the ellipse and its major axis length. The value is between 0 and 1.

Diameter: Scalar that specifies the diameter of a circle with the same area as the region. It is computed as [7]:

$$\sqrt{\frac{4Area}{\pi}}. \quad (11)$$

Major Axis Length: Scalar specifying the length (in pixels) of the major axis of the ellipse that has the same normalized second central moments as the region [7].

Minor Axis Length: Scalar specifying the length (in pixels) of the minor axis of the ellipse that has the same normalized second central moments as the region [7].

Since it is hard to determine which of these features are more suitable for classification, this research employed metaheuristic approach to select the optimal features for the classifier.

Particle Swarm Optimization

PSO is a population-based bio-inspired computational algorithm and is initialized by a randomly selected population called particles [5]. The particles are like 'a flock of birds' that collectively move in a search space in search of the best solution (global optimum) [5]. The objective function to be optimized is used to evaluate the fitness values of the particles in PSO. Also, the particles have velocities that direct their movement in the search space [22]. The position and velocity of particles are updated until the stopping criterion is met. The position of the particle is expressed by [1]:

$$x_i(t+1) = x_i(t) + v_i(t+1), \quad (12)$$

where x is the position of the particle i at time step t; $v_i(t+1)$ is the current velocity of the particle expressed as [1]:

$$v_i(t+1) = wv_i(t) + c_1 r_1 \left(pbest(t) - x_i(t)\right) + c_2 r_2 \left(gbest(t) - x_i(t)\right), \quad (13)$$

where w is the initial weight; c_1 is the learning rates for individual ability (cognitive); c_2 is the learning rates for social influence (group); r_1 and r_2 are random numbers between 0 and 1; *pbest* and *gbest* are the local and global best of the particles respectively.

The pseudocode for the PSO algorithm is shown below:

```
For each particle
   Initialize particle
END
Do
For each particle
    Calculate fitness value
    If the fitness value is better than the best fitness value
(pBest) in history
    set current value as the new pBest
End
    Choose the particle with the best fitness value of all the
particles as the gBest
For each particle
    Calculate particle velocity according equation (12)
   Update particle position according equation (13)
End
    While maximum iterations or minimum error criteria is not
     attained
```

Methodology

The following steps were adopted in this research:

(i) Pre-processing of the ultrasound images using an adaptive filter having the lowest MSE, and highest PSNR, image negative transformation, histogram equalization and morphological operations.
(ii) Segmentation of the image in (i) using an active contour without edge method.
(iii) Computation of the first order features, second order textural features and geometric features from the segmented regions.
(iv) Automatic selection of best features using PSO algorithm.
(v) Classification of follicles based on (iv) using a multilayer perceptron neural network classifier.
(vi) Evaluation of the results obtained in (v) in terms of accuracy, sensitivity and specificity.

Feature extraction phase

Here, multiple features, including second order features (Contrast, Correlation, Energy and Homogeneity), first order features (Mean, Standard Deviation, Kurtosis, Variance, Skew and Energy) and geometric features (Diameter, Area, Major Axis Length, Minor Axis Length) were extracted. Table 1 shows the respective features and their indexes.

Table 1. Features and their index

Index	Features	Index	Features	Index	Features
1	Diameter	6	Mean	11	Energy1
2	Area	7	Variance	12	Contrast
3	Eccentricity	8	Standard Deviation	13	Correlation
4	Major Axis Length	9	Skew	14	Energy2
5	Minor Axis Length	10	Kurtosis	15	Homogeneity

Selection of best features using PSO

To improve the accuracy of the system, the optimal features were selected using the PSO algorithm. This was based on tuning the ANN parameters until low MSE is achieved. The PSO feature selection algorithm is shown:

(i) Start
(ii) Set number of best features to be selected
(iii) Generate population of particles equal to the number of populations
(iv) Initialize particle positions and velocities
(v) Set local best fitness and local best positions
(vi) Set global best fitness and position equal to their minimum local best
(vii) Perform training of ANN
(viii) Evaluate fitness value of each particle
(ix) If current fitness is less than local best and global best
(x) Set global best fitness equal to current fitness, else
(xi) Update velocities and position
(xii) Stop if number of iterations is met

The fitness function for calculating the fitness values of the particles is given as [24]:

$$MSE = \frac{1}{N}\sum E^2, \tag{14}$$

where *MSE* is the mean square error; *N* is the number of tested samples; *E* is the error difference between the actual and the predicted class.

The best features selected serve as inputs to Multi-Layer Perceptron (MLP) ANN. The PSO parameters are shown in Table 2.

Table 2. PSO parameters

PSO parameters	Values
Swarm size	20
Maximum Iterations	100
Inertia Weight Damping Ratio	1
Maximum Variable size (VarMax)	1
Minimum Variable size (VarMin)	0
Inertia Weight	1
Velocity Maximum value (VelMax)	0.1(VarMax – VarMin)
Velocity Minimum value (VelMin)	–VelMax

Follicle detection algorithm
The following algorithm was adopted to identify the Region of Interest (ROI):

Algorithm 1:
1. Input the ultrasound image of the ovary
2. Denoise the ultrasound image using adaptive filters
3. Apply histogram equalization to enhance the clarity of the image
4. Negatively transform the image in Step 3
5. Remove small and spurious regions due to noise using morphological erosion
6. Apply Sobel filter to exaggerate the edges of regions of interest
7. Perform active contour without edges to segment the image and identify ROI
8. Repeat Step 1 to Step 7 for all the input images

MLP classification algorithm
The algorithm consists of the training and the testing phase which are explained in the following subsections:

Training and testing phase:
In the training phase, multiple features were extracted which were then used to train the MLP network. The following algorithm was adopted to extract second order features for the knowledge base and use the extracted features to train and test the MLP network:

Algorithm 2:
1. Input the ultrasound image of the ovary
2. Denoise the ultrasound image using adaptive filters
3. Apply histogram equalization to enhance the clarity of the image
4. Negatively transform the image in Step 3
5. Remove small and spurious regions due to noise using morphological erosion
6. Apply Sobel filter to exaggerate the edges of potential follicles
7. Perform active contour without edges to segment the image
8. Compute first order, second order texture and geometric features for each of the regions
9. Select the optimal features using PSO algorithm
10. Store the optimal features as knowledge base
11. Train the MLP network with the stored extracted features and save the network
12. Test the MLP network with the testing data (i.e., data that are unknown to the network) to classify the regions
13. Repeat Step 1 to Step 9 for all the input images

Fig. 1 represents the flowchart of the MLP training and testing algorithm. The input images are pre-processed. This is followed by segmenting the pre-processed image by applying the active contour without edge segmentation method. Then, the first order features, the second order texture features and the geometric features of each of the objects are computed and saved. Then, the optimal features are selected from the multiple extracted ones. These features are used to train the MLP network and subsequently, the network is saved. Further, unknown data are used to test the network and then, algorithm performance is evaluated using accuracy, sensitivity and specificity.

Materials and tools for the project
The materials needed for the successful completion of this project are discussed in the following subsections. The materials include image a dataset, an artificial neural network, and parameters for the evaluation of the project.

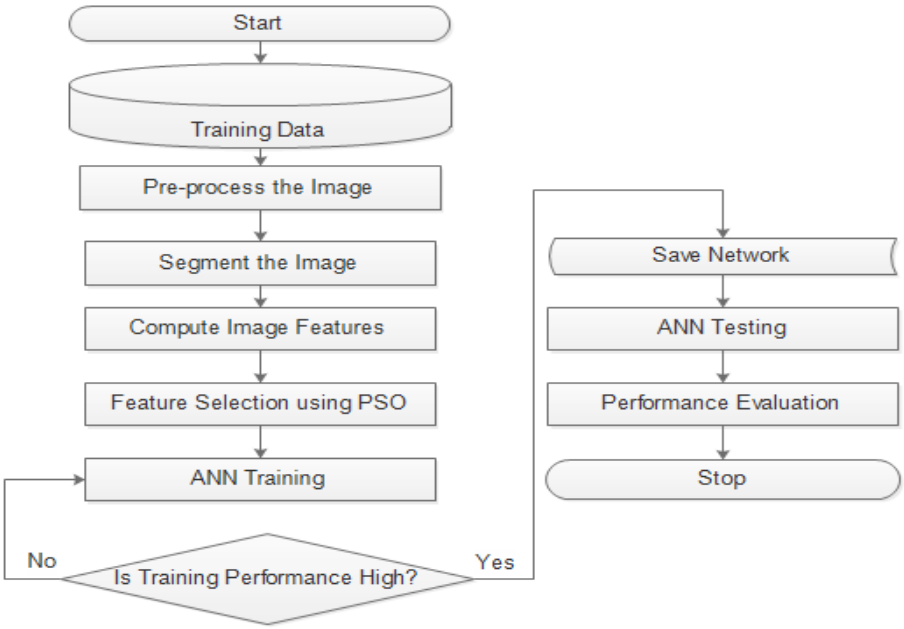

Fig. 1 Flowchart of MLP classification algorithm

Image dataset

For the purpose of this study and comparison, a twenty-five image dataset of ultrasound images of the ovary were obtained from the US National Library of Medicine, National Institute of Health (http://www.nlm.nih.gov).

ANN training and model selection

Multi-layer Neural Network models are trained. Each model is trained with a given number of input features selected by the PSO algorithm. The PSO algorithm determines the best number of features required for training a given model of ANN. The following parameters are used in designing the ANN models:

(i) Number of inputs (selected by PSO algorithm)
(ii) Multi-layer Neural Network is chosen because of its generalisation and fault tolerant ability
(iii) Numbers of neurons are chosen based on rule of thumbs which state that the number of hidden layer neurons is 2/3 of the size of the input layer [10]
(iv) The training function: A Levenberg-Marquet (trainlm) was chosen because it is faster and is able to attain low MSE on time as compared to the scaled conjugate gradient or another ANN training algorithm.
(v) Activation function: Linear function at the output layer and sigmoid function at the hidden layer sizes. This is because the expected output of the classification is either 0 or 1.

Performance evaluation

The performance of the classification algorithm is evaluated using the parameters accuracy, sensitivity, and specificity. All the parameters are expressed in terms of True Positive (*TP*), True Negative (*TN*), False Positive (*FP*) and False Negative (*FN*). Accuracy, sensitivity, and specificity are defined and expressed mathematically as [19]:

Accuracy (*AC*) is defined as the proportion of the correctly identified cases from the total number of cases and is given in this relation:

$$AC = \frac{TP + TN}{TP + FP + TN + FN}. \quad (15)$$

Sensitivity (*SE*) is defined as the measure of the ability of the method to identify abnormal cases and is given as:

$$SE = TP / (TP + FN). \quad (16)$$

Specificity (*SP*) is the measure of the ability of the method to identify normal cases and is given in a relation:

$$SP = TN / (TN + FP). \quad (17)$$

Results and discussion

This section presents and discusses the results of follicle detection and MLP classification algorithms.

Results of follicle detection algorithm

The performance of the follicle detection algorithm is evaluated using ultrasound images of the ovary. The result of the algorithm is shown in Fig. 2.

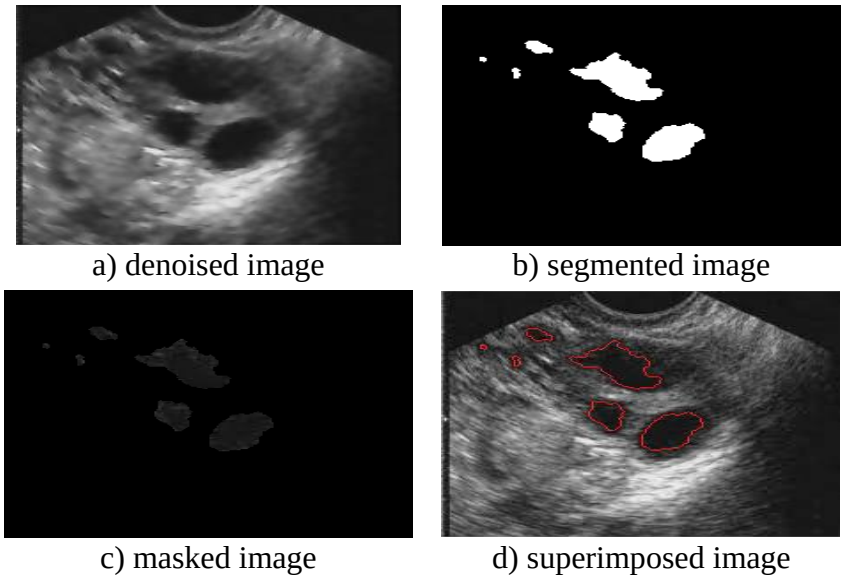

a) denoised image b) segmented image

c) masked image d) superimposed image

Fig. 2 Resultant images at different steps of the follicle detection algorithm

Fig. 2 depicts the resultant outputs of the follicle detection algorithm. This is to identify the ROI for further processing. Fig. 2a presents the original ultrasound images of the ovary. The outputs of the algorithm are represented in Fig. 2b-d. They are denoised, segmented, masked and superimposed images, respectively. The denoised images are the output of the application of the Lee filter; the segmented images are the output of the active contours without edge method; the masked images are the real texture of the segmented regions and finally, the superimposed images distinguish the detected regions from the background of the original images.

Table 3 shows specificity, sensitivity and accuracy values for different models of ANN, based on the number of features selected. Row nine, with twelve features and eight neurons, has the highest values of specificity (98%), sensitivity (100%) and accuracy (99%). The last column in the table represents the indexes of the selected optimal features.

Table 3. PSO-ANN classification results

S/N	Number of features	Number of hidden neurons	PSO-ANN algorithm	Index of selected features
			Specificity, Sensitivity, Accuracy	
1	4	2	96.6%, 93.5%, 95.0%	15, 12, 10, 13
2	5	3	96.0%, 82.9%, 88.3%	12, 1, 13, 14, 2
3	6	3	87.9%, 96.3%, 91.7%	10, 8, 9, 13, 5, 7
4	7	5	85.3%, 96.2%, 90.0%	14, 15, 7, 13, 1, 10, 12
5	8	5	87.9%, 96.3%, 91.7%	3, 11, 5, 2, 13, 8, 12, 1
6	9	6	83.3%, 100%, 90.0%	6, 13, 12, 11, 8, 1, 10, 14, 4
7	10	7	87.9%, 96.3%, 91.7%	12, 7, 1, 8, 15, 13, 10, 3, 11, 14
8	11	7	93.3%, 93.3%, 93.3%	11, 3, 9, 1, 13, 4, 14, 6, 7, 8, 2
9	12	8	96.8%, 100%, 98.3%	3, 6, 7, 13, 14, 12, 11, 15, 4, 8, 9, 10
10	13	9	90.6%, 96.4%, 93.3%	2, 14, 15, 10, 6, 12, 13, 8, 11, 4, 5, 9, 3
11	14	9	83.3%, 100%, 90.0%	7, 11, 9, 3, 12, 5, 10, 6, 1, 4, 2, 8, 14, 13
12	15	10	96.7%, 96.7%, 96.7%	15, 8, 5, 4, 14, 13, 11, 3, 10, 9, 1, 7, 6, 12, 2

Results of MLP classification algorithm

In this section, a three layers' neural network, namely, the input layer, the hidden layer and the output layer, is generated. The input layer has twelve inputs, selected by the PSO algorithm; the hidden layer has eight neurons, based on the rule of thumb [10].

The network configuration for this project is shown in Fig. 3. Presented ANN model was chosen after a series of experimenting with different models of the neural network. This model gives the highest accuracy compared to other models, as shown in Table 3. The performance of the designed neural network classifier is measured in terms of *AC*, *SE* and *SP*.

The confusion matrix shows the overall classification rate and accuracy of the network. A high classification rate and accuracy of the network signifies the ability of the network to correctly classify the two classes (i.e., follicles and non-follicles). The training dataset contains one hundred and sixty extracted features. One hundred are used for training and sixty are used for testing. The training dataset is divided into 80% training, 10% testing and 10% validation samples. This dataset is used to train the network until low MSE and less misclassification are achieved.

After training the network, the confusion matrix in Fig. 4 is plotted. The diagonal cells in green show the number of correctly classified cases and the off-diagonal cells in red show the number of misclassified cases. The first two ash cells to the top right show the percentages of the correctly classified follicles and non-follicles (100% and 98%) and the misclassified cases

(0% and 2%), respectively. The two ash cells to the bottom left show the percentages of the correctly predicted positive and negative cases (100% and 98%) and the percentages of the corresponding misclassified cases (0% and 2%). The blue cell in the bottom right shows the total percentage of the correctly classified cases (99%) and the percentage of the misclassified cases (1%). In all, the optimal features for the training data yield 99% *AC*, 100% *SE* and 98% *SP*.

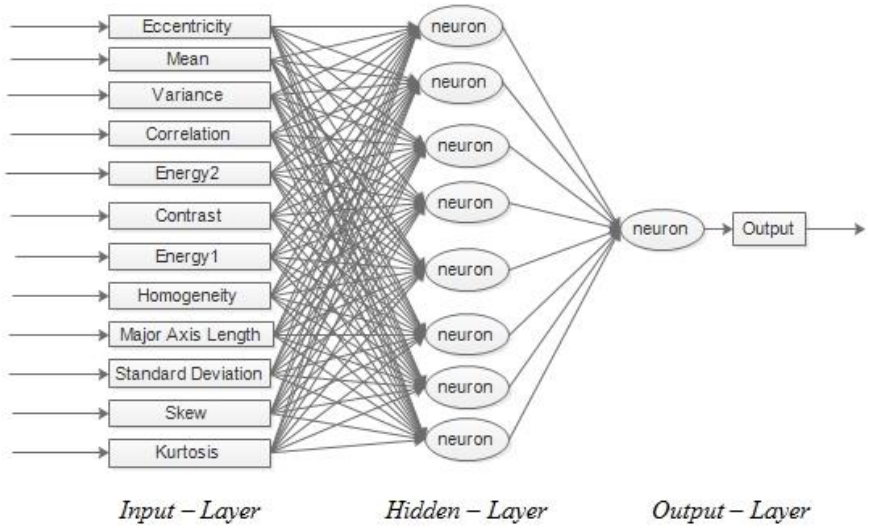

Fig. 3 Network configuration for the project

The result of the testing data determines that the optimal features yield an *AC* of 98.3%, 100% *SE* and 96.8% *SP* as shown in Fig. 5. The confusion matrix in Fig. 5 shows the overall performance of the testing data.

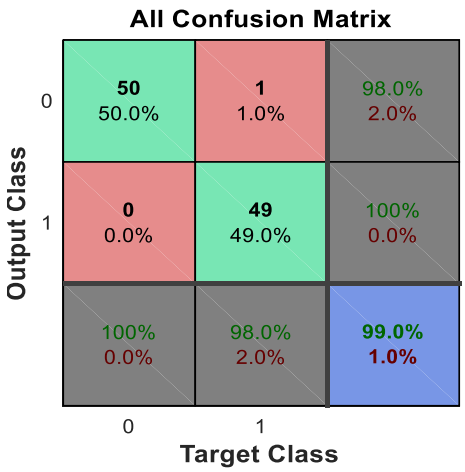

Fig. 4 Confusion matrix of GLCM training data

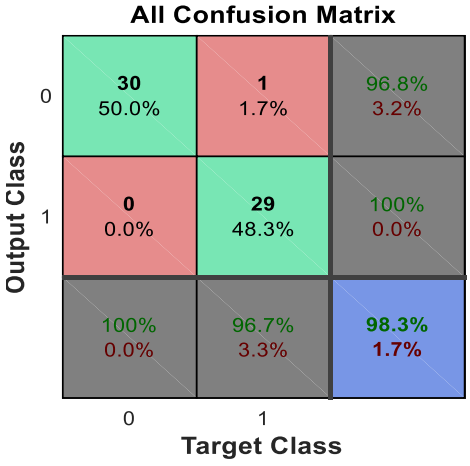

Fig. 5 Confusion matrix of GLCM testing data

The plot of the MSE against numbers of epochs is shown in Fig. 6. The best validation performance is 0.012068 at epoch 13. During training, the network divides the input and the target data into three different samples, which are training, validation and testing samples. The training samples are used to train the network and weights are adjusted according to its errors. The validation samples are used to measure network generalization and to halt training when the generalization stops improving. Further, testing samples are used to independently measure the performance of the network during and after training. The green line in Fig. 6

represents the validation, the blue line shows the training and the red line shows the testing. The green ring circle indicates the best point of validation performance of the network. And finally, at nineteen epochs, the generalization stops improving and consequently, the training is halted. This plot varies during retraining; the reason being that the input and the target data are divided randomly by the network for every retraining.

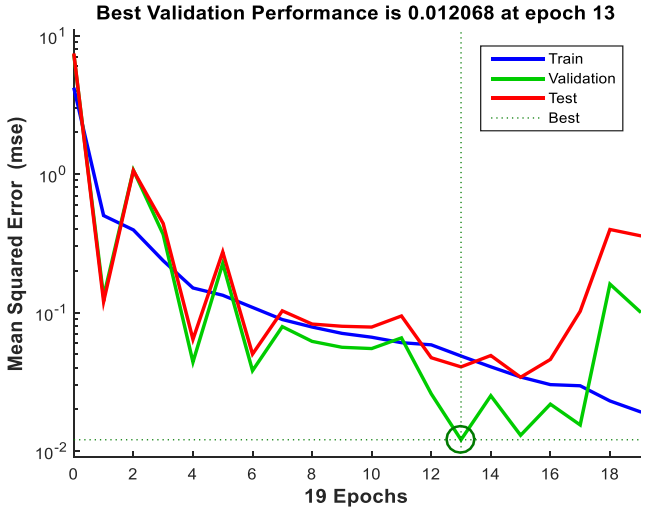

Fig. 6 Plot of validation performance of the network

Fig. 7 represents the command window for the training.

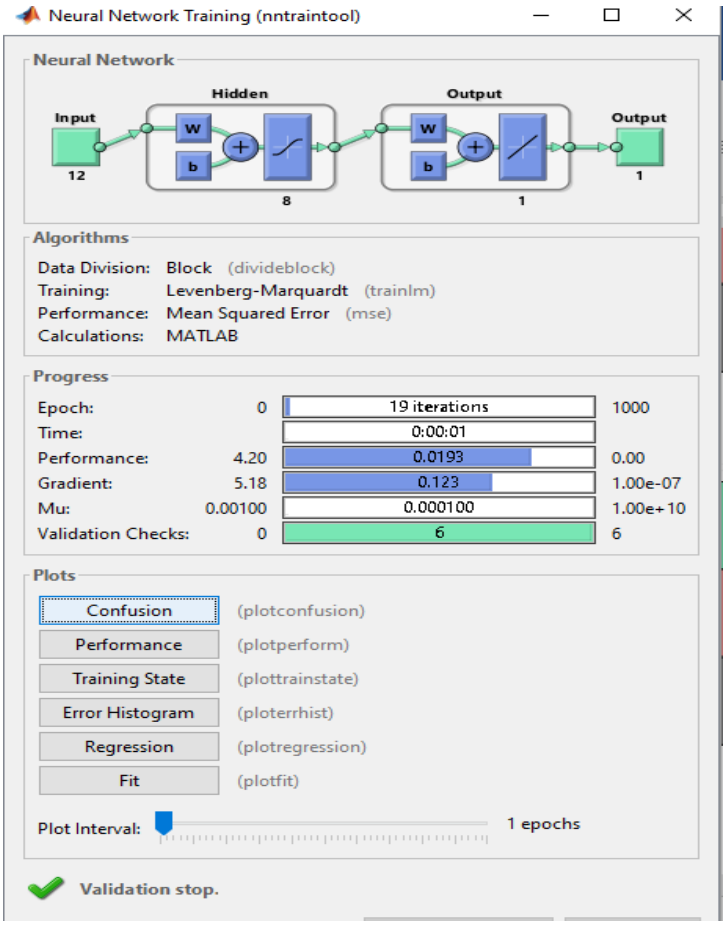

Fig. 7 Command window for the training

The interface shows some vital information pertaining to the training. It shows the network configuration for the project, the training algorithm, the numbers of iteration, the performance of the network as well as the validation checks for the training. Plots such as validation performance, training state and regression can be obtained directly from the interface.

Conclusion

In this paper, a follicle detection algorithm that comprises detection of the regions of interest and hybridized PSO-MLP classification algorithm, using optimal features and MLP, has been developed. The algorithm was developed in Matlab R2015a and the performance of the developed algorithm was evaluated in terms of accuracy, sensitivity and specificity of the network. The algorithm yielded an accuracy of 98.3%, 100% sensitivity and 96.8% specificity. The significance of these results is that the follicle detection rate is improved, which, consequently, improves the detection rate of follicle-related diseases such as PCOS. This implies that the developed algorithm is suitable to be employed for routine segmentation by medical experts.

References

1. Akbar H., N. Suryana, S. Sahib (2012). Controlling B-spline Snake Behaviour using Particle Swarm Optimization, Internationa Journal Bioautomation, 16(3), 179-186.
2. Cannistraci C. V., A. Abbas, X. Gao (2015). Median Modified Wiener Filter for Nonlinear Adaptive Spatial Denoising of Protein NMR Multidimensional Spectra, Scientific Report, 5:8017, doi: 10.1038/srep08017.
3. Chaurasia K., P. K. Garg (2013). A Brief Review on Texture Analysis Methods, Studies in Surveying and Mapping Science, 1(2), 1-9.
4. Fauser B. C., B. C., Tarlatzis, R. W. Rebar, R. S. Legro, A. H. Balen, R. Lobo, K. Barnhart (2012). Consensus on Women's Health Aspects of Polycystic Ovary syndrome (PCOS), Human Reproduction, 27(1), 14-24.
5. Ghamisi P., M. S. Couceiro, J. Benediktsson, N. M. F. Ferreira (2012). An Efficient Method for Segmentation of Images Based on Fractional Calculus and Natural Selection, Expert Systems with Applications, 39, 12407-12417.
6. Gonzalez R. C., R. E. Woods (2002). Digital Image Processing, New Jersey: Pearson Prentice-Hall Pearson Education, Inc.
7. Gonzalez R. C., R. E. Woods, S. L. Eddins (2004). Digital Image Processing Using MATLAB, New Jersey: Pearson Prentice-Hall Pearson Education, Inc.
8. Hamid B. A. (2011). Image Texture Analysis of Transvaginal Ultrasound in Monitoring Ovarian Cancer, Ph.D. Thesis, School of Engineering, Cardiff University.
9. Haralick R. E., K. Shanmugam, I. Dinstein (1973). Textural Features for Image Classification, IEEE Transactions on Systems, Man and Cybernetics, 3(6), 610-621.
10. Karsoliya S. (2012). Approximating Number of Hidden Layer Neurons in Multiple Hidden Layer BPNN Architecture, International Journal of Engineering Trends and Technology, 3(6), 713-717.
11. Karthikeyan S., N. Rengarajan (2014). Performance Analysis of Gray Level Co-occurrence Matrix Texture Features for Glaucoma Diagnosis, American Journal of Applied Sciences 11(2), 248-257.
12. Kaur D., Y. Kaur (2014). Intelligent Medical Image Segmentation using FCM, GA and PSO, International Journal of Computer Science and Information Technologies, 5(5), 6089-6093.
13. Kumar K. (2012). Artificial Neural Networks for Diagnosis of Kidney Stones Disease, International Journal of Information Technology and Computer Science, 7, 20-25.

14. Lingayat N. S., M. R. Tarambale (2013). A Computer Based Feature Extraction of Lung Nodule in Chest X-Ray Image, International Journal of Bioscience, Biochemistry and Bioinformatics, 3(6), 624-629.
15. Lujan M. E., D. R. Chizen, A. K. Peppin, A. Dhir, R. A. Pierson (2009). Assessment of Ultrasonographic Features of Polycystic Ovaries is Associated with Modest Levels of Inter-observer Agreement, Journal of Ovarian Research, 2, 1-6.
16. Mahmood N. H., S. N. Z. Ahmad, H. Hashim, S. N. N. Abdull-Rani (2012). Ovary Ultrasound Image Edge Detection Analysis: A Tutorial using MATLAB, International Journal of Engineering Research and Applications, 2(3), 1635-1642.
17. Malik F., B. Baharudin (2013). The Statistical Quantized Histogram Texture Features Analysis for Image Retrieval Based on Median and Laplacian Filters in the DCT Domain, The International Arab Journal of Information Technology, 10(6), 1-9.
18. Nithya R., B. Santhi (2011). Comparative Study on Feature Extraction Method for Breast Cancer Classification, Journal of Theoretical and Applied Information Technology, 33(2), 220-226.
19. Padma A., R. Sukanesh (2011). Automatic Classification and Segmentation of Brain Tumor in CT Images Using Optimal Dominant Gray Level Run Length Texture Features, International Journal of Advanced Computer Science and Applications, 2(10), 53-59.
20. Rezaei B., O. E. Ramos (2010). Scene Segmentation and Interpretation Image Characterization: Texture Analysis, Universitat de Girona, Spain.
21. Rini D. P., S. M. Shamsuddin, S. S. Yuhaniz (2011). Particle Swarm Optimization: Technique, System and Challenges, International Journal of Computer Applications, 14(1), 19-27.
22. Sathya P. D., R. Kayalvizhi (2010). Development of a New Optimal Multilevel Thresholding Using Improved Particle Swarm Optimization Algorithm for Image Segmentation, International Journal of Electronics Engineering, 2(1), 63-67.
23. Selvarajah S., S. R. Kodituwakku (2011). Analysis and Comparison of Texture Features for Content Based Image Retrieval, International Journal of Latest Trends in Computing, 2(1), 108-113.
24. Surchev S., S. Sotirov, W. Korneta (2013). Bio-inspired Artificial Intelligence: A Generalized Net Model of the Regularization Process in MLP, Internationa Journal Bioautomation, 17(3), 151-158.
25. Tegnoor J. R. (2012). Automated Ovarian Classification in Digital Ultrasound Images Using SVM, International Journal of Engineering Research & Technology, 1(6), 1-17.
26. Vause T. D. R., O. N. Ottawa, A. P. Cheung, B. C. Vancouver (2010). Ovulation Induction in Polycystic Ovary Syndrome, Journal of Obstetrics and Gynaecology Canada, 32(5), 495-502.
27. Wilson J. N., G. X. Ritter (2010). Handbook of Computer Vision Algorithms in Image Algebra, CRC Press.
28. York G., Y. Kim (1999). Ultrasound Processing and Computing: Review and Future Directions, Annual Review of Biomedical Engineering, 1(1), 559-581.

Omeiza Rabiu Isah, M.Sc. Student
E-mail: isah.rabiu@futminna.edu.ng

Omeiza Rabiu Isah received his B.Eng. degree in Electrical and Computer Engineering from the Federal University of Technology, Minna, Nigeria. Now, he is a Postgraduate student at the Department of Electrical and Computer Engineering, Ahmadu Bello University, Zaria, Nigeria. His current research interests include intelligent systems, telemedicine and biomedical imaging.

A. D. Usman, Ph.D.
E-mail: aliyu_d_usman@yahoo.com

Eng. Dr. A. D. Usman was born in Rigachikun, Kaduna State of Nigeria on January 1st, 1970. He acquired a Master of Engineering Degree from Bayero University Kano in 2006. He later proceeded to the prestigious University Putra Malaysia where he obtained his Ph.D. in Electrical Engineering (Biomed and Microwave) Engineering in 2011. He has more than 53 national and international publications from reputable journals and conferences. He is a member of the Institute of Electrical and Electronic Engineers, the Nigerian Society of Engineers, the Nigerian Institute of Physics, the National Solar Energy of Nigeria and a registered engineer with the Council for Regulation of Engineering Practice in Nigeria.

A. M. S. Tekanyi, Ph.D.
E-mail: amtekanyi@abu.edu.ng

Dr. A. M. S. Tekanyi obtained his B.Eng. (Hons) degree in Electrical Engineering from the University of Sierra-Leone, Freetown in 1990, his M.Sc. Degree in Computer Networks from the Middlesex University, London in 2001, and his Ph.D. degree in Electrical Engineering from Ahmadu Bello University, Zaria, in 2014. His Ph.D. research thesis is Telecommunication Engineering based and Centered on WLAN Bandwidth Improvement. His research interests are focused on telecommunications engineering, with an emphasis on finding out problems of wireless and WLAN networks and their resolutions, in particular, finding out factors affecting efficient bandwidth utilization, channel congestion, traffic delay, and traffic loss. He is also interested in computer engineering, e.g., computer network security research area and related researches in this area.